H_2 Formation and Excitation in the Stephan's Quintet Galaxy-Wide Shock

Pierre Guillard[1], François Boulanger[1], Guillaume Pineau des Forêts[1], Phil Appleton[2]

ABSTRACT

Spitzer has detected extremely powerful ($L_{H_2} > 10^{41}$ erg s^{-1}), shock-powered, mid-IR H_2 emission towards the Stephan's Quintet (SQ) galaxy group (Appleton et al. 06). This is the first time an almost pure H_2 line spectrum has been seen in an extragalactic object. The luminosity in the H_2 lines exceeds the X-ray luminosity. How can we explain the formation and excitation of such a huge amount of warm ($T \geqslant 185$ K) molecular gas ($M_{H_2} \sim 4 \times 10^7 M_\odot$) coexisting with a X-ray emitting plasma?

We present a scenario where the molecular gas is formed in the shock. The pre-shock gas is assumed to be inhomogeneous. Schematically, low density volume filling pre-shock gas ($n_H \lesssim 0.01$ cm^3) is shocked at the collision speed ($\sim 1\,000$ km s^{-1} for SQ) and becomes a dust-free X-ray emitting plasma. The hot gas pressure induces slower shocks in diffuse gas clouds. This gas ($n_H \gtrsim 0.1$ cm^3) is heated at lower temperatures and dust survives. In the context of the SQ shock, this gas had time to cool and become molecular. Then, because all the mechanical energy is not still dissipated, the relative motions between the gas phases lead to energetic exchanges through the plasma-clouds interface. The observations show that this energy dissipation is very efficient to excite H_2 in its rotational lines. We phenomenologically model this turbulence by secondary low velocity shocks driven into these clouds. These shocks are able to heat the newly-formed H_2 and produce the observed unusual strong H_2 to X-ray luminosity ratio.

This contribution is a preliminary presentation of a model to be fully described in Guillard et al. 2008, in preparation.

Subject headings: ISM: general – ISM: dust, extinction – ISM: molecules – Atomic processes – Molecular processes – Shock waves – Galaxies: interactions

1. Introduction

Recently, Spitzer IRS (Infra-Red Spectrometer) observations led to the unexpected detection of extremely bright mid-IR ($L > 10^{41}$erg s^{-1}) H_2 rotational line emission from warm gas towards

[1]Institut d'Astrophysique Spatiale, UMR 8617, CNRS, Université Paris-Sud 11, France

[2]Nasa *Herschel* Science Center, Caltech, Pasadena, USA

the group-wide shock in Stephan's Quintet (hereafter SQ) (see Fig. 1 and Appleton et al. 2006). This first result was quickly followed by the detection of bright H_2 line emission from more distant galaxies (Egami et al. 2007, Ogle et al. 2007) and from the NGC 1275 and NGC 4696 cooling flows (Johnstone et al. 2007). These H_2-bright galaxies may represent an important signature of galaxy evolution, but this unusual emission accompanied by little (or no) star formation has not yet been explained. Because of the absence or relative weakness of star forming signatures (dust features, ionized gas lines) in the mid-infrared Spitzer spectra, the H_2 emission must be powered by large-scale shocks, associated with galaxy interactions but also possibly with gas infall and/or AGN feedback.

SQ is a nearby (94 Mpc) group of galaxies where observations of the HI and HII gas distribution and kinematics provide a clear astrophysical context (Fig. 1). A wide (5×25 kpc) shock is creating by a galaxy (NGC 7318b) colliding into a tidal tail at a relative velocity of $\sim 1\,000$ km s^{-1}. We summarize here a scenario (P. Guillard et al. 2008, in prep.) which aim at explaining how H_2 can be formed and excited in such a shock. We use the Stephan's Quintet group as a close template to test our model. In section 2 we draw the overall picture of the scenario we are considering and we argue that the density inhomogeneities of the pre-shock gas create a multiphasic post-shock medium. In sect. 3, we give our main results about the gas cooling and the dust survival, with emphasis on the critical time scales. We also briefly discuss our modeling of H_2 formation and emission in the post-shock gas, and compare our results to the recent *Spitzer* observations of SQ.

2. Description of the scenario: a picture of galaxy-wide shocks

The Stephan's Quintet is a unique object for studying large-scale shocks and the origin of the H_2 emission. The luminosity in the H_2 lines measured by IRS onboard *Spitzer* exceeds by a factor ~ 2 the surface brightness in X-rays, and contains 30% of the total bolometric luminosity. It implies the presence of $3 \times 10^7 M_\odot$ of H_2 gas at 185 K. *A priori*, two possibilities can be evoked to explain the observed H_2 luminosity. The unusual bright H_2 emission can be either accounted for by:

1. the excitation of pre-existing dense and massive molecular clouds when they cross the shock.
2. molecular gas that form in the shock.

In the first possibility, the shock compression is expected to trigger the collapse of gravitationally bound clouds and thereby a burst of star formation (e.g. Jog & Solomon 1992). The absence of photo-ionization and thereby massive star formation in the shocked region (Xu et al. 2003) rules out this scenario. In our scenario we examine the second possibility, which imply that the H_2 emission is tracing the formation of large quantities of molecular gas.

Chandra and *XMM* observations indicate that the X-ray emitting gas has a temperature of $T_X \sim 5 \times 10^6$ K and an average proton density of $n_X \sim 0.02\,\mathrm{cm}^{-3}$ (Trinchieri et al. 2003,

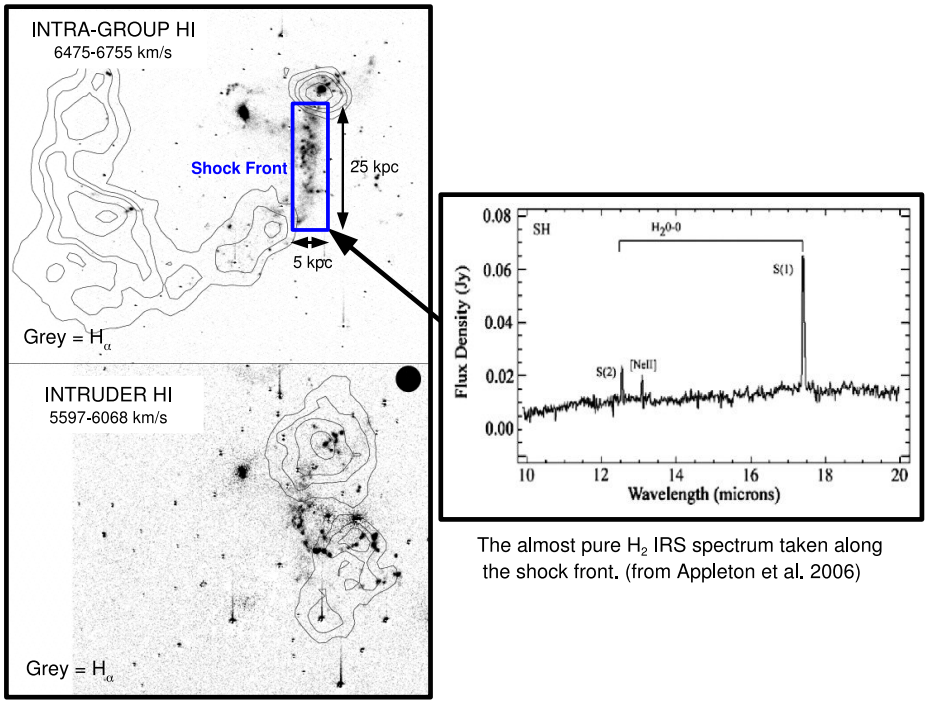

The almost pure H_2 IRS spectrum taken along the shock front. (from Appleton et al. 2006)

Fig. 1.— The Stephan's Quintet colliding gas flows: HI and H_α observations of SQ, separated in both SQ tidal stream and intruder velocity components. The HI 21 cm radio contours are integrated in two velocity intervals (top: 6475-6755 km/s; bottom: 5597-6068 km/s) superposed on an H_α interference filter image (same velocity ranges than HI). Images on the left are adapted from Sulentic et al. 2001. The mid-IR Spitzer IRS (Short High mode) taken by Appleton et al. along the shock front (blue rectangle) is shown on the right.

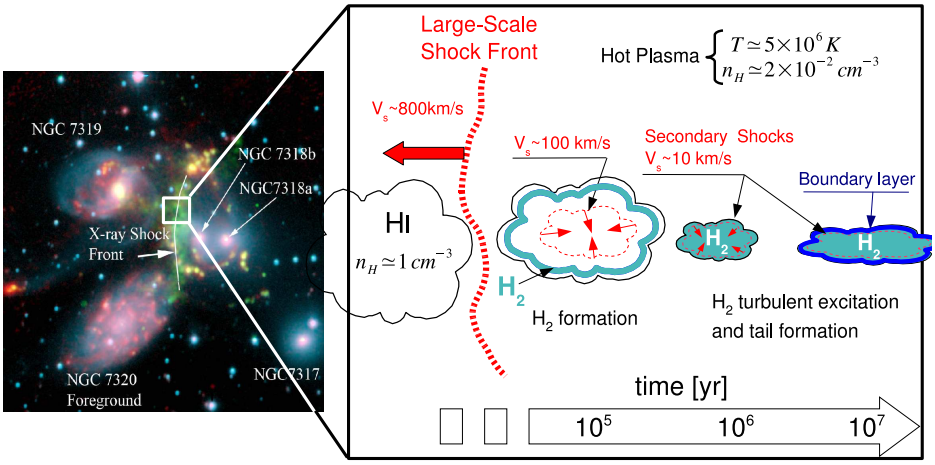

Fig. 2.— A schematic picture of a galaxy-wide shock in an inhomogeneous medium. *Left:* A three color image of the Stephan's Quintet system (visible in blue, Hα in green, and *Spitzer* IRAC 8-μm in red. *Right:* Schematic evolution of a shocked intergalactic gas cloud. In the teneous medium, the shock is propagating fast ($\sim$ 800 km s^{-1}), whereas in the HI cloud a lower velocity shock is driven, leading to the formation of a H_2 shell in the post-shock gas, and then of a molecular dense clump. Then, because all the kinetical energy is not dissipated in one large-scale shock, low velocity ($\sim$ 10 km s^{-1}) secondary shocks are driven into the freshly formed molecular gas. In the meanwhile, the relative motion of the global flow and the clumps produces extended structures (tails). The timescale is indicated at the bottom.

2005). Therefore, the cooling time scale of this hot plasma is $t_{\rm cool} \sim 10^8$ yr (Gnat & Sternberg, 2007), which is one order of magnitude greater than the collision age between the intruder galaxy NGC 7318b and the intergalactic medium (hereafter IGM), $t_{\rm coll} \sim 5{\times}10^6$ yr, for a relative velocity of $\sim$ 1 000 km s^{-1} and a shock width of 5 kpc. This suggests that the coexistence of molecular gas with a X-ray emitting plasma cannot be explained with a high-velocity shock hitting an homogeneous and tenuous gas.

Indeed, the pre-shock gas is made of galactic matter (tidal tail + galactic disk) and is expected to be *inhomogeneous*, with diffuse HI gas embedded in a teneous warm/hot volume filling plasma. The collision speed is the shock speed only in the low density volume filling gas. Shocks propagate slower into the HI gas (e.g. McKee & Cowie 1975). In the context of the SQ shock, we will show that this gas has time to cool and become molecular in less than 10^6 yr. Then, a next step follows during the next $\sim 10^7$ yr: the molecular clumps interact with the global flow to form extended structures such as tails or filaments (Dyson et al. 1993). The newly-formed H_2 is likely to be excited by energetic exchanges between the tenuous plasma and the molecular clouds. Turbulence is expected to play a fundamental role in the excitation of H_2 at the boundary layers of these filaments. Based on the study of the H_2 excitation diagram, we will examine the effect of low-velocity secondary shocks driven into the H_2 gas. Fig. 2 describes schematically the scenario we are testing.

Our model quantifies the four crucial time scales[1] introduced above as a function of the initial density of the pre-shock gas and the post-shock temperature (i.e. the shock velocity). Today, the initial shock has already gone through the colliding gas flows, and we are looking at the evolution of the post-shock gas. Its local physical state depends on how these time scales are arranged with respect to each other, and this ordering depends on the local physical conditions of the gas.

3. A model of the multiphasic post-shock medium: critical time scales

3.1. Gas cooling and formation of H_2

Four main physical ingredients are considered in our model: the cooling of the hot ($T > 10^4$ K) plasma, the cooling of the gas after its recombination, the formation of molecular gas, and the dust destruction in the shocked medium, which plays a role in the first three processes. Since the large-scale shock imprints a high post-shock pressure in the X-ray emitting plasma ($P_{\rm ps}/k_{\rm B} \sim 2.3 \times 10^5$ cm^{-3} K), we assume that the gas cooling is isobaric. To sum up, the thermodynamics and the chemistry of the cooling post-shock gas are modeled in two steps:

1. From the post-shock temperature ($T_{\rm ps} \simeq 10^7$ K for a shock velocity of $V_s = 800$ km s^{-1}) to 10^4 K the gas cooling is calculated by integrating the energy balance equation, using a cooling

[1]The dynamical time scale or collision age, $t_{\rm coll}$, the dust destruction by sputtering, $t_{\rm sput}$, the gas cooling, $t_{\rm cool}$, and the H_2 formation time scale.

function which is dynamically computed and includes both atomic processes as well as dust cooling and dust destruction.

2. From 10^4 K to ~ 10 K, the model of Flower et al. 2003 was used to compute the steady-state cooling and chemistry of the gas, in particular the formation of H_2.

We show the temperature profiles for an isobaric cooling on Fig. 3 (*left*), from the post-shock temperature down to 10^4 K, for different shock velocities, from 100 to 1 000 km s^{-1}. This corresponds to a range of pre-shock densities of ~ 0.2 to 2×10^{-3} cm^{-3}, respectively. The final gas density at 10^4 K is $n_{\rm H} \sim 10\,{\rm cm}^{-3}$. We have indicated in Fig. 3 (*left*) the collision age (dynamical time scale), $t_{\rm coll} \sim 5 \times 10^6$ yr. This roughly materializes the time at which we are observing the shocked gas. When a large-scale shock is propagating into an inhomogeneous medium, a range of shock velocities, and thereby of temperatures, is introduced in the post-shock gas. Fig. 3 shows that the gas which is shocked at $V_s \lesssim 500$ km s^{-1} had time to cool down to 10^4 K. We show (Guillard et al. 2008, in prep; Fig. 4) that this gas had time to become molecular. On the contrary, the gas shocked at $V_s \gtrsim 700$ km s^{-1} remains the X-ray emitting plasma at $\sim 5 \times 10^6$ K because the cooling time scale is greater than the collision age. According to our results about dust destruction, this plasma is predicted to be dust-free.

Fig. 3 (*right*) shows the dust lifetime (dashed line) as a function of the post-shock temperature and initial post-shock density. Each post-shock temperature corresponds to a given shock velocity. The dust lifetime has a minimum of $\sim 5 \times 10^5$ yrs around $T_{\rm ps} \sim 1.2 \times 10^6$ K, which shows that the dust destruction is the most efficient for these physical conditions (shock velocity of ~ 300 km s^{-1} and initial post-shock density of $\sim 8 \times 10^{-2}$ cm^{-3}). When one decreases the post-shock temperature (or increases the initial pre-shock density), the dust lifetime increases because the sputtering rate drops below the threshold ($\sim 10^6$ K). On the contrary, the dust lifetime increases towards high temperatures because the yield[2] is roughly constant but the density decreases. The gas cooling time scale is overplotted (solid line) in Fig. 3. The crossing of the dust lifetime and the cooling time scale demarcates the 3 phases of the post-shock gas: the H_2 phase at low post-shock temperatures ($n_{\rm H} \gtrsim 0.2\,{\rm cm}^{-3}$), the hot plasma phase at very high post-shock temperatures ($n_{\rm H} \lesssim 0.04\,{\rm cm}^{-3}$), and an intermediate zone which may contain HII or HI gas.

The chemical abundances profiles in the post-shock gas during the cooling of the gas for $T < 10^4$ K are given in Fig. 4 as a function of the flow time. The 1-D code of Flower et al. has been adapted to an isobaric cooling for a single fluid. The initial conditions are set from the results of the previous cooling calculations i.e. $T = 10^4$ K, $n_{\rm H} = 10\,{\rm cm}^{-3}$. At 10^4 K the gas is roughly 90% ionized. Fig. 4 shows that, from the moment when the gas attains 10^4 K, it takes only $\sim 2 \times 10^5$ yrs to form H_2. The H_2 formation gives rise to a "plateau" in the temperature profile around 200 K. At this point, the energy released by the H_2 formation is approximatively counterbalanced by the cooling due to O, H_2O and CO. Therefore, provided that the gas that has cooled down to 10^4 K is

[2]Number of atoms ejected from the grains surface per incident particle.

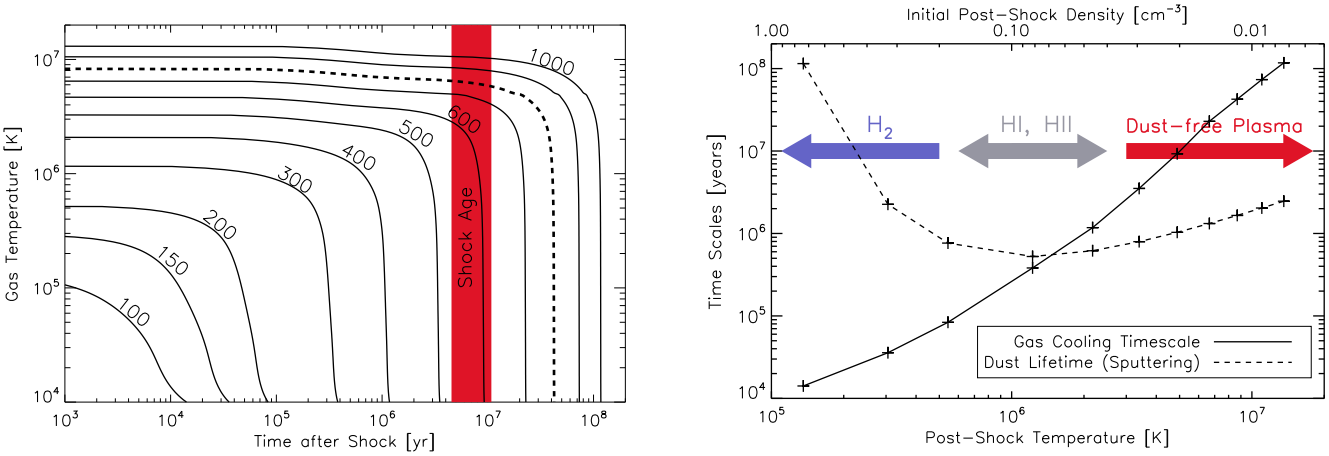

Fig. 3.— The multiphasic post-shock medium. *Left:* Evolution of the gas temperature with time at constant pressure, from the post-shock temperature to 10^4 K for different shock velocities V_s [km s^{-1}]. The dashed line is for V_s = 800 km s^{-1}, which corresponds to the hot gas of Stephan's Quintet case. The red vertical line at 10^7 yr indicates the order of magnitude of the collision time scale between the intruding galaxy NGC 7318b and the IGM. *Right:* Dust destruction (dashed line) and gas cooling (full line) time scales in the post-shock gas of the Stephan's Quintet intra-group medium. These time scales have to be compared with the SQ shock age ($\sim 10^7$ yr) and the H_2 formation time scale ($\sim 5 \times 10^5$ yrs). Below 10^6 K, the gas has time to cool and become molecular before dust is detroyed. The gas cooling time scale is computed at the post-shock temperature.

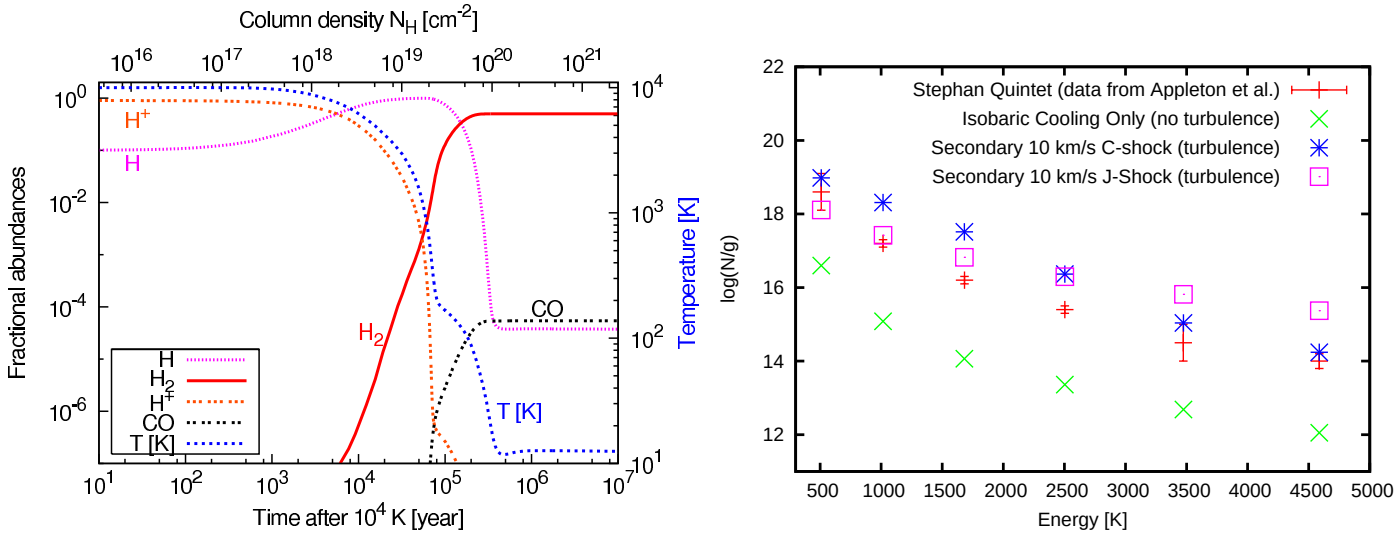

Fig. 4.— Our modelling of H_2 formation and excitation in the post-shock gas. *Left:* Temperature (blue line, labeled on the right side) and abundances profiles relative to $n_{\rm H}$ for a model in which, initially, $n_{\rm H} = 10$ cm^{-3}, $T = 10^4$ K and $B = 5\mu$G. The final density is 4×10^4 cm^{-3}, for a temperature of 12 K. *Right:* The H_2 excitation diagram computed for three different models: (green) Isobaric Cooling from $n_{\rm H} = 10\,{\rm cm}^{-3}$, $T = 10^4$ K (same as the plot on the left). (blue) Secondary 10 km/s C-shock in the newly-formed post-shock molecular gas. (magenta) Secondary 10 km/s J-shock in the newly-formed post-shock molecular gas. (red) Comparison with the Stephan's Quintet data of Appleton et al. (2006)

dusty, i.e. the denser pre-shock gas that has been shocked to lower velocities, H_2 reforms efficiently in the post-shock gas.

3.2. Turbulent excitation of H_2

However, Fig. 4 show that H_2 forms lately along the cooling curve, when the gas has already cooled down to $T \lesssim 200\,\mathrm{K}$. This temperature is too low to produce the observed excitation of the H_2 rotational lines (Fig. 4, *left*, green points). As introduced in section 2, the newly-formed dense molecular gas is expected to be subsequently excited by turbulence on a longer time scale.

This is essentially due to the fact that all the kinetical energy of the shock is not dissipated at once. Indeed, we evaluated that the time scale of dissipation of the total kinetical energy of the shock ($t_{\rm diss} \sim 3 \times 10^8$ yr) is one order of magnitude larger than the collision age ($t_{\rm coll} \sim 5 \times 10^6\,\mathrm{yr}$). Indeed, the observed H_2 rotational linewidths show a high-velocity dispersion (~ 870 km s^{-1}) for the warm H_2 gas (Appleton et al. 2006). This indicates that we are in presence of mass-loaded flows with relative motion between the gas phases. The physical mechanism which drives the dissipation of the flow kinetic energy is not understood, but the observations tell us that it excites H_2 in its low-J lines. The H_2 emission may be powered by energetic exchanges at the interface with the hot plasma. At this stage, our model is phenomenological: we consider that secondary shocks occur in the boundary layer of the filaments which are created by the relative motion of the global flow with respect to the clumps.

We have modeled the effect of low velocity (~ 5 to 20 km s^{-1}) secondary shocks, induced by the turbulence, on the molecular content formed in the post-shock gas. Our results, particularly the H_2 surface brightness and excitation, are in agreement with SQ observations. We find that the observed surface brightness of the H_2 S(0) to S(3) rotational lines falls close to modeled one, and in between 10 km s^{-1} C- and J-type shocks. The calculated excitation diagram of H_2 show that a 10 km s^{-1} J-shock into the newly-formed molecular gas reproduces well the high energy levels (Fig. 4, *left*). On the contrary, a 10 km s^{-1} C-shock matches the lower energy rotational levels of H_2. This indicates that we may have a combination of both J- and C-type shocks, or non-stationary shocks in the turbulent boundary layer of the "H_2 fingers".

4. Summary

We have quantified the relevant time scales for the description of the SQ wide shock and explored a scenario which may explain why we see an unusually bright mid-IR H_2 emission from the galaxy-wide shock in Stephan's Quintet and almost no star formation: a large scale shock overruns an inhomogeneous pre-shock medium, leading to a clumpy (multi-phase) post-shock gas where a large amount of H_2 is formed. In ISM words, the shock is converting the HI gas into molecular gas. The hot interstellar medium (HIM) remains HIM. Qualitatively, most of the shock

energy is stored in the tenuous hot gas (where the shock velocity is higher), but dense gas, radiates most of the turbulent energy through H_2 lines because the cooling time is shorter (density is higher).

The physics of galaxy-wide shocks briefly described here is likely to be universal in lots of H_2-luminous galaxies. The understanding of these physical processes in the Stephan's Quintet will undoubtedly help us to understand what powers the strong H_2 emission in the new set of H_2-bright objects discovered by *Spitzer*.

REFERENCES

Appleton, P. N., Xu, K. C., Reach, W., et al. 2006, ApJ, 639, L51

Dyson, J. E., Hartquist, T. W., & Biro, S. 1993, MNRAS, 261, 430

Egami, E., Rieke, G. H., Fadda, D., & Hines, D. C. 2006, ApJ, 652, L21

Flower, D. R., Le Bourlot, J., Pineau des Forêts, G., & Cabrit, S. 2003, MNRAS, 341, 70

Gnat & Sternberg, 2007, ApJS, 168, 213

Guillard, P., Boulanger, F., Pineau des Forêts, G., Appleton, P.N., 2008, A&A, in prep.

Johnstone, R. M., Hatch, N. A., Ferland, G. J., et al. 2007, MNRAS, 382, 1246

McKee, C. F. & Cowie, L. L. 1975, ApJ, 195, 715

Ogle, P., Antonucci, R., Appleton, P. N., & Whysong, D. 2007, ApJ, 668, 699

Sulentic, J. W., Rosado, M., Dultzin-Hacyan, D., et al. 2001, AJ, 122, 2993

Trinchieri, G., Sulentic, J., Breitschwerdt, D., & Pietsch, W. 2003, A&A, 401, 173

Trinchieri, G., Sulentic, J., Pietsch, W., & Breitschwerdt, D. 2005, A&A, 444, 697

Xu, C. K., Lu, N., Condon, J. J., Dopita, M., & Tuffs, R. J. 2003, ApJ, 595, 665